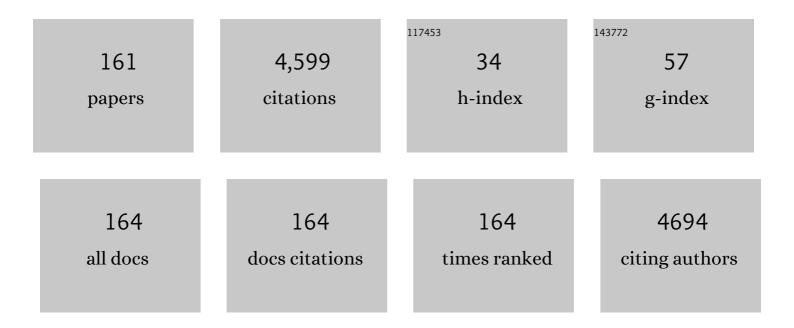
List of Publications by Year in descending order

Source: https://exaly.com/author-pdf/1587683/publications.pdf Version: 2024-02-01



ΙΟΗΝΙΤΛΝΝΕΡ

#	Article	IF	CITATIONS
1	Determinants of Enzyme Thermostability Observed in the Molecular Structure of Thermus aquaticus d-Glyceraldehyde-3-phosphate Dehydrogenase at 2.5 Ã Resolution,. Biochemistry, 1996, 35, 2597-2609.	1.2	216
2	X-ray crystal structures of native HIV-1 capsid protein reveal conformational variability. Science, 2015, 349, 99-103.	6.0	212
3	Redox Regulation of Protein Tyrosine Phosphatases: Structural and Chemical Aspects. Antioxidants and Redox Signaling, 2011, 15, 77-97.	2.5	149
4	A structurally conserved water molecule in Rossmann dinucleotide-binding domains. Protein Science, 2009, 11, 2125-2137.	3.1	138
5	Structural biology of proline catabolism. Amino Acids, 2008, 35, 719-730.	1.2	136
6	Bioinformatics Methods for Mass Spectrometry-Based Proteomics Data Analysis. International Journal of Molecular Sciences, 2020, 21, 2873.	1.8	134
7	High-resolution structure of humanD-glyceraldehyde-3-phosphate dehydrogenase. Acta Crystallographica Section D: Biological Crystallography, 2006, 62, 290-301.	2.5	108
8	The Proline Cycle As a Potential Cancer Therapy Target. Biochemistry, 2018, 57, 3433-3444.	1.2	107
9	Flavin Reductase P:  Structure of a Dimeric Enzyme That Reduces Flavin,. Biochemistry, 1996, 35, 13531-13539.	1.2	98
10	Structure of the proline dehydrogenase domain of the multifunctional PutA flavoprotein. Nature Structural Biology, 2003, 10, 109-114.	9.7	96
11	Structure and Kinetics of Monofunctional Proline Dehydrogenase from Thermus thermophilus. Journal of Biological Chemistry, 2007, 282, 14316-14327.	1.6	88
12	Artificial intelligence in the prediction of protein–ligand interactions: recent advances and future directions. Briefings in Bioinformatics, 2022, 23, .	3.2	78
13	Structures of theEscherichia coliPutA Proline Dehydrogenase Domain in Complex with Competitive Inhibitorsâ€,â€į. Biochemistry, 2004, 43, 12539-12548.	1.2	74
14	A comparative study of time dependent quantum mechanical wave packet evolution methods. Journal of Chemical Physics, 1992, 96, 2077-2084.	1.2	73
15	Ab initio study of proton transfer in [H3Nâ^'Hâ^'NH3]+ and [H3Nâ^'Hâ^'OH2]+. Chemical Physics Letters, 1990, 175, 282-288.	1.2	70
16	Structure of Francisella tularensis AcpA. Journal of Biological Chemistry, 2006, 281, 30289-30298.	1.6	67
17	Structures of the PutA peripheral membrane flavoenzyme reveal a dynamic substrate-channeling tunnel and the quinone-binding site. Proceedings of the National Academy of Sciences of the United States of America, 2014, 111, 3389-3394.	3.3	63
18	Structural Basis of the Transcriptional Regulation of the Proline Utilization Regulon by Multifunctional PutA. Journal of Molecular Biology, 2008, 381, 174-188.	2.0	62

#	Article	IF	CITATIONS
19	Crystal structure of the bifunctional proline utilization A flavoenzyme from <i>Bradyrhizobium japonicum</i> . Proceedings of the National Academy of Sciences of the United States of America, 2010, 107, 2878-2883.	3.3	59
20	The Biological Buffer Bicarbonate/CO ₂ Potentiates H ₂ O ₂ -Mediated Inactivation of Protein Tyrosine Phosphatases. Journal of the American Chemical Society, 2011, 133, 15803-15805.	6.6	57
21	The Three-Dimensional Structural Basis of Type II Hyperprolinemia. Journal of Molecular Biology, 2012, 420, 176-189.	2.0	57
22	Crystal structure of an antigen-binding fragment bound to single-stranded DNA 1 1Edited by I. A. Wilson. Journal of Molecular Biology, 2001, 314, 807-822.	2.0	56
23	Structure, function, and mechanism of proline utilization A (PutA). Archives of Biochemistry and Biophysics, 2017, 632, 142-157.	1.4	56
24	Redox-Induced Changes in Flavin Structure and Roles of Flavin N(5) and the Ribityl 2â€~-OH Group in Regulating PutAâ^'Membrane Bindingâ€,‡. Biochemistry, 2007, 46, 483-491.	1.2	51
25	Structure, mechanism, and dynamics of UDP-galactopyranose mutase. Archives of Biochemistry and Biophysics, 2014, 544, 128-141.	1.4	49
26	Identification and Characterization of the DNA-binding Domain of the Multifunctional PutA Flavoenzyme. Journal of Biological Chemistry, 2004, 279, 31171-31176.	1.6	46
27	Unusual folded conformation of nicotinamide adenine dinucleotide bound to flavin reductase P. Protein Science, 1999, 8, 1725-1732.	3.1	45
28	Steady-state kinetic mechanism of the proline:ubiquinone oxidoreductase activity of proline utilization A (PutA) from Escherichia coli. Archives of Biochemistry and Biophysics, 2011, 516, 113-120.	1.4	43
29	Resolving the cofactor-binding site in the proline biosynthetic enzyme human pyrroline-5-carboxylate reductase 1. Journal of Biological Chemistry, 2017, 292, 7233-7243.	1.6	42
30	Determination of protein oligomeric structure from smallâ€angle Xâ€ray scattering. Protein Science, 2018, 27, 814-824.	3.1	40
31	Crystal structures of the DNA-binding domain ofEscherichia coliproline utilization A flavoprotein and analysis of the role of Lys9 in DNA recognition. Protein Science, 2006, 15, 2630-2641.	3.1	38
32	First Evidence for Substrate Channeling between Proline Catabolic Enzymes. Journal of Biological Chemistry, 2015, 290, 2225-2234.	1.6	37
33	Structural Biology of Proline Catabolic Enzymes. Antioxidants and Redox Signaling, 2019, 30, 650-673.	2.5	37
34	The Structure of the Proline Utilization A Proline Dehydrogenase Domain Inactivated by N-Propargylglycine Provides Insight into Conformational Changes Induced by Substrate Binding and Flavin Reduction,. Biochemistry, 2010, 49, 560-569.	1.2	36
35	Diethylaminobenzaldehyde Is a Covalent, Irreversible Inactivator of ALDH7A1. ACS Chemical Biology, 2015, 10, 693-697.	1.6	36
36	Structural Basis of Substrate Recognition by Aldehyde Dehydrogenase 7A1. Biochemistry, 2015, 54, 5513-5522.	1.2	36

#	Article	IF	CITATIONS
37	The Structure of the Antibiotic Deactivating, N-hydroxylating Rifampicin Monooxygenase. Journal of Biological Chemistry, 2016, 291, 21553-21562.	1.6	36
38	Exploring structurally conserved solvent sites in protein families. Proteins: Structure, Function and Bioinformatics, 2006, 64, 404-421.	1.5	34
39	Solution structure of Ca ²⁺ â€free rat βâ€parvalbumin (oncomodulin). Protein Science, 2007, 16, 1914-1926.	3.1	33
40	Crystal Structures and Small-angle X-ray Scattering Analysis of UDP-galactopyranose Mutase from the Pathogenic Fungus Aspergillus fumigatus. Journal of Biological Chemistry, 2012, 287, 9041-9051.	1.6	33
41	AutoCryoPicker: an unsupervised learning approach for fully automated single particle picking in Cryo-EM images. BMC Bioinformatics, 2019, 20, 326.	1.2	33
42	Crystal Structures and Kinetics of Monofunctional Proline Dehydrogenase Provide Insight into Substrate Recognition and Conformational Changes Associated with Flavin Reduction and Product Release. Biochemistry, 2012, 51, 10099-10108.	1.2	31
43	MRSAD: using anomalous dispersion from S atoms collected at Cuâ€Kα wavelength in molecular-replacement structure determination. Acta Crystallographica Section D: Biological Crystallography, 2003, 59, 1731-1736.	2.5	30
44	A Conserved Active Site Tyrosine Residue of Proline Dehydrogenase Helps Enforce the Preference for Proline over Hydroxyproline as the Substrate. Biochemistry, 2009, 48, 951-959.	1.2	30
45	Structural Studies of Yeast Δ ¹ -Pyrroline-5-carboxylate Dehydrogenase (ALDH4A1): Active Site Flexibility and Oligomeric State. Biochemistry, 2014, 53, 1350-1359.	1.2	30
46	DeepCryoPicker: fully automated deep neural network for single protein particle picking in cryo-EM. BMC Bioinformatics, 2020, 21, 509.	1.2	30
47	Molecular Dynamics Simulations of NAD+in Solution. Journal of the American Chemical Society, 1999, 121, 8637-8644.	6.6	29
48	Crystal structure of a bacterial phosphoglucomutase, an enzyme involved in the virulence of multiple human pathogens. Proteins: Structure, Function and Bioinformatics, 2011, 79, 1215-1229.	1.5	29
49	Crystal structure of rat α-parvalbumin at 1.05 à resolution. Protein Science, 2004, 13, 1724-1734.	3.1	28
50	Evidence for Structural Plasticity of Heavy Chain Complementarity-determining Region 3 in Antibody–ssDNA Recognition. Journal of Molecular Biology, 2005, 347, 965-978.	2.0	28
51	Proline: Mother Nature's cryoprotectant applied to protein crystallography. Acta Crystallographica Section D: Biological Crystallography, 2012, 68, 1010-1018.	2.5	28
52	Evidence for Hysteretic Substrate Channeling in the Proline Dehydrogenase and Δ1-Pyrroline-5-carboxylate Dehydrogenase Coupled Reaction of Proline Utilization A (PutA). Journal of Biological Chemistry, 2014, 289, 3639-3651.	1.6	28
53	Conformations of nicotinamide adenine dinucleotide (NAD+) in various environments. , 2000, 13, 27-34.		27
54	Characterization of recombinant Francisella tularensis acid phosphatase A. Protein Expression and Purification, 2006, 45, 132-141.	0.6	27

#	Article	IF	CITATIONS
55	Unique structural features and sequence motifs of proline utilization A (PutA). Frontiers in Bioscience - Landmark, 2012, 17, 556.	3.0	27
56	Structures of Proline Utilization A (PutA) Reveal the Fold and Functions of the Aldehyde Dehydrogenase Superfamily Domain of Unknown Function. Journal of Biological Chemistry, 2016, 291, 24065-24075.	1.6	27
57	Solution structure of Ca ²⁺ â€free rat αâ€parvalbumin. Protein Science, 2008, 17, 431-438.	3.1	25
58	Structural Basis for the Inactivation of Thermus thermophilus Proline Dehydrogenase by <i>N-</i> Propargylglycine [,] . Biochemistry, 2008, 47, 5573-5580.	1.2	25
59	Identification of the NAD(P)H Binding Site of Eukaryotic UDP-Galactopyranose Mutase. Journal of the American Chemical Society, 2012, 134, 18132-18138.	6.6	25
60	Anti-insulin antibody structure and conformation. II. Molecular dynamics with explicit solvent. Biopolymers, 1992, 32, 23-32.	1.2	24
61	Structural Determinants of Oligomerization of Δ1-Pyrroline-5-Carboxylate Dehydrogenase: Identification of a Hexamerization Hot Spot. Journal of Molecular Biology, 2013, 425, 3106-3120.	2.0	24
62	Structural basis of substrate selectivity of Δ1-pyrroline-5-carboxylate dehydrogenase (ALDH4A1): Semialdehyde chain length. Archives of Biochemistry and Biophysics, 2013, 538, 34-40.	1.4	24
63	Empirical power laws for the radii of gyration of protein oligomers. Acta Crystallographica Section D: Structural Biology, 2016, 72, 1119-1129.	1.1	24
64	A modified landau-teller model for vibrational relaxation of small molecular ions. Chemical Physics Letters, 1987, 138, 495-502.	1.2	23
65	Floquet analysis of the far-infrared dissociation of a Morse oscillator. Physical Review A, 1989, 40, 4054-4064.	1.0	23
66	A computer-based approach to teaching quantum dynamics. Journal of Chemical Education, 1990, 67, 917.	1.1	23
67	Crystal Structures ofTrypanosoma cruziUDP-Galactopyranose Mutase Implicate Flexibility of the Histidine Loop in Enzyme Activation. Biochemistry, 2012, 51, 4968-4979.	1.2	23
68	Covalent Allosteric Inactivation of Protein Tyrosine Phosphatase 1B (PTP1B) by an Inhibitor–Electrophile Conjugate. Biochemistry, 2017, 56, 2051-2060.	1.2	22
69	In crystallo screening for proline analog inhibitors of the proline cycle enzyme PYCR1. Journal of Biological Chemistry, 2020, 295, 18316-18327.	1.6	22
70	<i>In Crystallo</i> Capture of a Covalent Intermediate in the UDP-Galactopyranose Mutase Reaction. Biochemistry, 2016, 55, 833-836.	1.2	21
71	Structure and characterization of a class 3B proline utilization A: Ligand-induced dimerization and importance of the C-terminal domain for catalysis. Journal of Biological Chemistry, 2017, 292, 9652-9665.	1.6	21
72	Molecular dynamics simulations and rigid body (TLS) analysis of aspartate carbamoyltransferase: Evidence for an uncoupled R state. Protein Science, 1993, 2, 927-935.	3.1	20

#	Article	IF	CITATIONS
73	Structural and Biochemical Characterization of Aldehyde Dehydrogenase 12, the Last Enzyme of Proline Catabolism in Plants. Journal of Molecular Biology, 2019, 431, 576-592.	2.0	20
74	Structure, biochemistry, and gene expression patterns of the proline biosynthetic enzyme pyrroline-5-carboxylate reductase (PYCR), an emerging cancer therapy target. Amino Acids, 2021, 53, 1817-1834.	1.2	20
75	Cloning, purification and crystallization ofBacillus anthracisclass C acid phosphatase. Acta Crystallographica Section F: Structural Biology Communications, 2006, 62, 705-708.	0.7	19
76	Functional Role for the Conformationally Mobile Phenylalanine 223 in the Reaction of Methylenetetrahydrofolate Reductase from <i>Escherichia coli</i> . Biochemistry, 2009, 48, 7673-7685.	1.2	19
77	Targeting UDP-Galactopyranose Mutases from Eukaryotic Human Pathogens. Current Pharmaceutical Design, 2013, 19, 2561-2573.	0.9	19
78	Kinetic and Structural Characterization of Tunnel-Perturbing Mutants in <i>Bradyrhizobium japonicum</i> Proline Utilization A. Biochemistry, 2014, 53, 5150-5161.	1.2	19
79	Structure of Bacterial Luciferase β2 Homodimer:  Implications for Flavin Binding,. Biochemistry, 1997, 36, 665-672.	1.2	18
80	Energetics of OCP1–OCP2 complex formation. Biophysical Chemistry, 2008, 134, 64-71.	1.5	18
81	Evidence That the C-Terminal Domain of a Type B PutA Protein Contributes to Aldehyde Dehydrogenase Activity and Substrate Channeling. Biochemistry, 2014, 53, 5661-5673.	1.2	18
82	Characterization of a Unique Class C Acid Phosphatase from <i>Clostridium perfringens</i> . Applied and Environmental Microbiology, 2009, 75, 3745-3754.	1.4	17
83	Small-angle X-ray Scattering Studies of the Oligomeric State and Quaternary Structure of the Trifunctional Proline Utilization A (PutA) Flavoprotein from Escherichia coli. Journal of Biological Chemistry, 2011, 286, 43144-43153.	1.6	17
84	Involvement of the β3-α3 Loop of the Proline Dehydrogenase Domain in Allosteric Regulation of Membrane Association of Proline Utilization A. Biochemistry, 2013, 52, 4482-4491.	1.2	17
85	Crystal Structure of a High-Affinity Variant of Rat α-Parvalbuminâ€. Biochemistry, 2004, 43, 10008-10017.	1.2	16
86	Structure of an anti-DNA fab complexed with a non-DNA ligand provides insights into cross-reactivity and molecular mimicry. Proteins: Structure, Function and Bioinformatics, 2004, 57, 269-278.	1.5	15
87	Desulfovibrio desulfuricans G20 Tetraheme Cytochrome Structure at 1.5Ã and Cytochrome Interaction with Metal Complexes. Journal of Molecular Biology, 2006, 358, 1314-1327.	2.0	15
88	Inactivation of protein tyrosine phosphatases by dietary isothiocyanates. Bioorganic and Medicinal Chemistry Letters, 2015, 25, 4549-4552.	1.0	15
89	Crystal Structure of Aldehyde Dehydrogenase 16 Reveals Trans-Hierarchical Structural Similarity and a New Dimer. Journal of Molecular Biology, 2019, 431, 524-541.	2.0	15
90	Inhibition, crystal structures, and in-solution oligomeric structure of aldehyde dehydrogenase 9A1. Archives of Biochemistry and Biophysics, 2020, 691, 108477.	1.4	15

#	Article	IF	CITATIONS
91	Probing a hydrogen bond pair and the FAD redox properties in the proline dehydrogenase domain of Escherichia coli PutA. Biochimica Et Biophysica Acta - Proteins and Proteomics, 2004, 1701, 49-59.	1.1	14
92	Impact of DNA Hairpin Folding Energetics on Antibody–ssDNA Association. Journal of Molecular Biology, 2007, 374, 1029-1040.	2.0	14
93	Structure of Recombinant Haemophilus Influenzae e (P4) Acid Phosphatase Reveals a New Member of the Haloacid Dehalogenase Superfamily,. Biochemistry, 2007, 46, 11110-11119.	1.2	14
94	Recognition of Nucleoside Monophosphate Substrates by Haemophilus influenzae Class C Acid Phosphatase. Journal of Molecular Biology, 2010, 404, 639-649.	2.0	14
95	Biophysical investigation of type A PutAs reveals a conserved core oligomeric structure. FEBS Journal, 2017, 284, 3029-3049.	2.2	14
96	Structure and function of a flavin-dependent S-monooxygenase from garlic (Allium sativum). Journal of Biological Chemistry, 2020, 295, 11042-11055.	1.6	14
97	Crystallization and preliminary crystallographic analysis of the proline dehydrogenase domain of the multifunctional PutA flavoprotein fromEscherichia coli. Acta Crystallographica Section D: Biological Crystallography, 2001, 57, 1925-1927.	2.5	13
98	Conservation of Functionally Important Global Motions in an Enzyme Superfamily across Varying Quaternary Structures. Journal of Molecular Biology, 2012, 423, 831-846.	2.0	13
99	Contribution to catalysis of ornithine binding residues in ornithine N5-monooxygenase. Archives of Biochemistry and Biophysics, 2015, 585, 25-31.	1.4	13
100	Impact of disease-Linked mutations targeting the oligomerization interfaces of aldehyde dehydrogenase 7A1. Chemico-Biological Interactions, 2017, 276, 31-39.	1.7	13
101	Structural Evidence for Rifampicin Monooxygenase Inactivating Rifampicin by Cleaving Its Ansa-Bridge. Biochemistry, 2018, 57, 2065-2068.	1.2	13
102	Trapping conformational states of a flavin-dependent N-monooxygenase in crystallo reveals protein and flavin dynamics. Journal of Biological Chemistry, 2020, 295, 13239-13249.	1.6	13
103	Impaired folate binding of serine hydroxymethyltransferase 8 from soybean underlies resistance to the soybean cyst nematode. Journal of Biological Chemistry, 2020, 295, 3708-3718.	1.6	13
104	Crystal Structures of the Histidine Acid Phosphatase from Francisella tularensis Provide Insight into Substrate Recognition. Journal of Molecular Biology, 2009, 394, 893-904.	2.0	12
105	Solution structures of polcalcin Phl p 7 in three ligation states: Apoâ€, hemiâ€Mg ²⁺ â€bound, and fully Ca ²⁺ â€bound. Proteins: Structure, Function and Bioinformatics, 2013, 81, 300-315.	1.5	12
106	A Super-Clustering Approach for Fully Automated Single Particle Picking in Cryo-EM. Genes, 2019, 10, 666.	1.0	12
107	Crystallization of AcpA, a respiratory burst-inhibiting acid phosphatase from Francisella tularensis. Biochimica Et Biophysica Acta - Proteins and Proteomics, 2005, 1752, 107-110.	1.1	11
108	Substrateâ€dependent dynamics of UDPâ€galactopyranose mutase: Implications for drug design. Protein Science, 2013, 22, 1490-1501.	3.1	11

#	Article	IF	CITATIONS
109	Multiple functionalities of reduced flavin in the non-redox reaction catalyzed by UDP-galactopyranose mutase. Archives of Biochemistry and Biophysics, 2017, 632, 59-65.	1.4	11
110	NAD ⁺ promotes assembly of the active tetramer of aldehyde dehydrogenase 7A1. FEBS Letters, 2018, 592, 3229-3238.	1.3	11
111	The role of rotation in the vibrational relaxation of diatomic molecules. Chemical Physics, 1988, 119, 307-324.	0.9	10
112	Quaternary structure, conformational variability and global motions of phosphoglucosamine mutase. FEBS Journal, 2011, 278, 3298-3307.	2.2	10
113	Covalent Modification of the Flavin in Proline Dehydrogenase by Thiazolidine-2-Carboxylate. ACS Chemical Biology, 2020, 15, 936-944.	1.6	10
114	Far IR dissociation of a highly excited Morse oscillator. Chemical Physics Letters, 1988, 149, 503-509.	1.2	9
115	Crystal structure and tartrate inhibition of Legionella pneumophila histidine acid phosphatase. Archives of Biochemistry and Biophysics, 2015, 585, 32-38.	1.4	9
116	Structural Basis for the Substrate Inhibition of Proline Utilization A by Proline. Molecules, 2018, 23, 32.	1.7	9
117	SAXSDom: Modeling multidomain protein structures using smallâ€angle Xâ€ray scattering data. Proteins: Structure, Function and Bioinformatics, 2020, 88, 775-787.	1.5	9
118	Disease variants of human Δ1-pyrroline-5-carboxylate reductase 2 (PYCR2). Archives of Biochemistry and Biophysics, 2021, 703, 108852.	1.4	9
119	Three crystal forms of the bifunctional enzyme proline utilization A (PutA) fromBradyrhizobium japonicum. Acta Crystallographica Section F: Structural Biology Communications, 2008, 64, 949-953.	0.7	8
120	Structure of Avian Thymic Hormone, a High-Affinity Avian β-Parvalbumin, in the Ca2+-Free and Ca2+-Bound States. Journal of Molecular Biology, 2010, 397, 991-1002.	2.0	8
121	Contributions of Unique Active Site Residues of Eukaryotic UDP-Galactopyranose Mutases to Substrate Recognition and Active Site Dynamics. Biochemistry, 2014, 53, 7794-7804.	1.2	8
122	Structural Determinants of Flavin Dynamics in a Class B Monooxygenase. Biochemistry, 2020, 59, 4609-4616.	1.2	8
123	Crystallization of a newly discovered histidine acid phosphatase fromFrancisella tularensis. Acta Crystallographica Section F: Structural Biology Communications, 2006, 62, 32-35.	0.7	7
124	Crystallization of recombinantHaemophilus influenzaee(P4) acid phosphatase. Acta Crystallographica Section F: Structural Biology Communications, 2006, 62, 464-466.	0.7	7
125	Solution structures of chicken parvalbumin 3 in the Ca ²⁺ â€free and Ca ²⁺ â€bound states. Proteins: Structure, Function and Bioinformatics, 2011, 79, 752-764.	1.5	7
126	SAXS fingerprints of aldehyde dehydrogenase oligomers. Data in Brief, 2015, 5, 745-751.	0.5	7

#	Article	IF	CITATIONS
127	Importance of the C-Terminus of Aldehyde Dehydrogenase 7A1 for Oligomerization and Catalytic Activity. Biochemistry, 2017, 56, 5910-5919.	1.2	7
128	Discovery of the Membrane Binding Domain in Trifunctional Proline Utilization A. Biochemistry, 2017, 56, 6292-6303.	1.2	7
129	Flavinâ€N5 Covalent Intermediate in a Nonredox Dehalogenation Reaction Catalyzed by an Atypical Flavoenzyme. ChemBioChem, 2018, 19, 53-57.	1.3	7
130	Structural and biochemical consequences of pyridoxineâ€dependent epilepsy mutations that target the aldehyde binding site of aldehyde dehydrogenase ALDH 7A1. FEBS Journal, 2020, 287, 173-189.	2.2	7
131	Cautionary Tale of Using Tris(alkyl)phosphine Reducing Agents with NAD ⁺ -Dependent Enzymes. Biochemistry, 2020, 59, 3285-3289.	1.2	7
132	Cloning, purification and crystallization ofThermus thermophilusproline dehydrogenase. Acta Crystallographica Section F: Structural Biology Communications, 2005, 61, 737-739.	0.7	6
133	Engineering a trifunctional proline utilization A chimaera by fusing a DNA-binding domain to a bifunctional PutA. Bioscience Reports, 2016, 36, .	1.1	6
134	Structural analysis of pathogenic mutations targeting Glu427 of ALDH7A1, the hot spot residue of pyridoxineâ€dependent epilepsy. Journal of Inherited Metabolic Disease, 2020, 43, 635-644.	1.7	6
135	Structural analysis of prolines and hydroxyprolines binding to the l-glutamate-Î ³ -semialdehyde dehydrogenase active site of bifunctional proline utilization A. Archives of Biochemistry and Biophysics, 2021, 698, 108727.	1.4	6
136	Biochemical Characterization of the Two-Component Flavin-Dependent Monooxygenase Involved in Valanimycin Biosynthesis. Biochemistry, 2021, 60, 31-40.	1.2	6
137	Structure-affinity relationships of reversible proline analog inhibitors targeting proline dehydrogenase. Organic and Biomolecular Chemistry, 2022, 20, 895-905.	1.5	6
138	Crystallization and molecular-replacement studies of a recombinant antigen-binding fragment complexed with single-stranded DNA. Acta Crystallographica Section D: Biological Crystallography, 2000, 56, 1007-1011.	2.5	5
139	Identification of a Conserved Histidine As Being Critical for the Catalytic Mechanism and Functional Switching of the Multifunctional Proline Utilization A Protein. Biochemistry, 2017, 56, 3078-3088.	1.2	5
140	N-Propargylglycine: a unique suicide inhibitor of proline dehydrogenase with anticancer activity and brain-enhancing mitohormesis properties. Amino Acids, 2021, 53, 1927-1939.	1.2	5
141	Structural and Biochemical Characterization of the Flavin-Dependent Siderophore-Interacting Protein from <i>Acinetobacter baumannii</i> . ACS Omega, 2021, 6, 18537-18547.	1.6	5
142	Preliminary crystallographic analysis of glyceraldehyde 3-phosphate dehydrogenase from the extreme thermophile Thermus aquaticus. Acta Crystallographica Section D: Biological Crystallography, 1994, 50, 744-748.	2.5	4
143	Detection ofL-lactate in polyethylene glycol solutions confirms the identity of the active-site ligand in a proline dehydrogenase structure. Acta Crystallographica Section D: Biological Crystallography, 2004, 60, 985-986.	2.5	4
144	Crystal Structure of the D94S/G98E Variant of Rat α-Parvalbumin. An Explanation for the Reduced Divalent Ion Affinityâ€. Biochemistry, 2005, 44, 10966-10976.	1.2	4

#	Article	IF	CITATIONS
145	Crystal structure and immunogenicity of the class C acid phosphatase from Pasteurella multocida. Archives of Biochemistry and Biophysics, 2011, 509, 76-81.	1.4	4
146	Synchrotron-based macromolecular crystallography module for an undergraduate biochemistry laboratory course. Journal of Applied Crystallography, 2016, 49, 2235-2243.	1.9	4
147	Structural basis for the stereospecific inhibition of the dual proline/hydroxyproline catabolic enzyme ALDH4A1 by transâ€4â€hydroxy‣â€proline. Protein Science, 2021, 30, 1714-1722.	3.1	4
148	Expression, purification and crystallization of class C acid phosphatases fromFrancisella tularensisandPasteurella multocida. Acta Crystallographica Section F: Structural Biology Communications, 2009, 65, 226-231.	0.7	3
149	Steric Control of the Rate-Limiting Step of UDP-Galactopyranose Mutase. Biochemistry, 2018, 57, 3713-3721.	1.2	3
150	Probing the function of a ligand-modulated dynamic tunnel in bifunctional proline utilization A (PutA). Archives of Biochemistry and Biophysics, 2021, 712, 109025.	1.4	3
151	Crystallization of Phi29 Spindle-Shaped Nano-Bar Anti-Receptor with Glycosidase Domain. Journal of Nanoscience and Nanotechnology, 2007, 7, 2616-2622.	0.9	2
152	Structural basis of the inhibition of class C acid phosphatases by adenosine 5′â€phosphorothioate. FEBS Journal, 2011, 278, 4374-4381.	2.2	2
153	Expression, purification and crystallization of an atypical class C acid phosphatase fromMycoplasma bovis. Acta Crystallographica Section F: Structural Biology Communications, 2011, 67, 1296-1299.	0.7	2
154	EF5 Is the High-Affinity Mg2+ Site in ALG-2. Biochemistry, 2016, 55, 5128-5141.	1.2	2
155	Redox Modulation of Oligomeric State in Proline Utilization A. Biophysical Journal, 2018, 114, 2833-2843.	0.2	2
156	Photoinduced Covalent Irreversible Inactivation of Proline Dehydrogenase by S-Heterocycles. ACS Chemical Biology, 2021, 16, 2268-2279.	1.6	2
157	2 PutA and proline metabolism. , 2012, , 31-56.		1
158	Impact of missense mutations in the ALDH7A1 gene on enzyme structure and catalytic function. Biochimie, 2021, 183, 49-54.	1.3	1
159	Optimisation of Neuraminidase Expression for Use in Drug Discovery by Using HEK293-6E Cells. Viruses, 2021, 13, 1893.	1.5	1
160	Evidence for Proline Catabolic Enzymes in the Metabolism of Thiazolidine Carboxylates. Biochemistry, 2021, 60, 3610-3620.	1.2	0
161	Kinetics of human pyrroline-5-carboxylate reductase in l-thioproline metabolism. Amino Acids, 2021, 53, 1863-1874.	1.2	0